Importance of body surface potential field representation fidelity: analysis of beat-to-beat repolarization measurements

György Kozmann[1,2], Kristóf Haraszti[2]

[1]Department of Information Systems, University of Pannonia, Veszprém,
[2]Department of Bioengineering, Research Institute for Technical Physics and Materials Science of the Hungarian Academy of Sciences, Budapest, Hungary

ABSTRACT

Objective: According to previous studies, the complex substrate of malignant arrhythmias needs a detailed spatio-temporal noninvasive characterization of low-amplitude dynamic changes in beat-to-beat cardiac repolarization.

Methods: Body surface potential map (BSPM) records were taken on 14 healthy male and female subjects (age 20-80 years) and on 6 ventricular arrhythmia patients, 4 of them with implanted cardioverter defibrillators (ICD). Records were taken continuously, for 5 minutes, in resting, supine position. Beat-to-beat QRST integral maps, Karhunen-Loève coefficient time-series (KL_i, *i=1-12*), RR and nondipolarity index (NDI) time-series were computed.

Results: The first order statistical properties of the spatio-temporal variability of subsequent QRST integral maps were characterized by the box and whiskers plot of their KLi components. The SD^2/M^2 (KL_i amplitude variance/mean signal energy) values of the QRST integral maps in the normal group ranged between 0.0057 and 0.008 (i.e. $0.075 \leq SD/M \leq 0.089$). In ICD patients SD^2/M^2 values went up to 0.021-0.069 (i.e: $0.14 \leq SD/M \leq 0.26$). Autocorrelation functions revealed that while in normal subjects only 5-20% of the total power had white noise character, the rest was bandwidth-limited noise. In ICD patients the weight of white noise component increased considerably. The higher the SD/M relative KL variability, the higher and more frequent NDI spikes were.

Conclusions: Beat-to-beat dynamics of white noise components of high resolution BSPMs are able to stratify arrhythmia vulnerability. The temporal distribution of extreme NDI spike formations is random; the frequency is associated with the relative KL component noise levels. *(Anadolu Kardiyol Derg 2007: 7 Suppl 1; 5-7)*

Key words: repolarization disparity, nondipolarity index, body surface potential maps, arrhythmia vulnerability, heart rate variability

Introduction

According to basic electrophysiological experiments, arrhythmia vulnerability is associated with elevated disparity of ventricular repolarization. Several possible mechanisms were studied that may result in the elevation of arrhythmia vulnerability. Noninvasive methods were recommended for the detection of pathological repolarization disparity, including measurements performed on low-noise averaged majority beats, time- and frequency-domain heart rate variability measurements, and spatial QT dispersion estimates (1-5). Other approaches try to get information from the beat-to-beat lability of QT duration in electrocardiogram (ECG) leads (6, 7), as well as from the vulnerability changes evoked by single or multiple premature stimuli (8-10).

In this paper, the theoretically well understood QRST integral maps and some derived scalar parameters extracted from the subsequent beats are used to reveal malignant changes in a train of beats (11). Special attention has been paid to the beat-to-beat spatio-temporal QRST integral dynamics in sinus rhythm.

Methods

We assessed experimentally the first and second order statistical properties of noninvasive spatio-temporal repolarization (gradient of action potential area) dynamics by the use of long BSPM records taken on 14 healthy male and female (NOR) subjects and in 6 documented ventricular arrhythmia (ARR) patients, with a typical length of 5 minutes. Map data were recorded from 64 chest positions according to the electrode layout suggested in Amsterdam.

Data processing started with the identification of individual beats, high-precision determination of QRS fiducial points, and classification of beat patterns according to their QRS shape. Subsequently, Q_{onset}, S_{end} and T_{end} points were marked in each heart cycle by an automatic procedure, but the final position of these points was adjusted by human intervention. After a linear base-line adjustment from the measured 64 signals, unipolar ECG signals were estimated in 128 un-measured chest locations of the 192-lead arrangement introduced at the CVRTI, Salt Lake City. The procedure of signal estimations followed the principle suggested by Lux et al. (12). Finally, QRST integrals were computed from the data of the 192-lead system.

For the detailed quantitative representation of beat-to-beat spatial repolarization patterns, QRST integral maps and difference maps (indicating departure from the average integral distributions) were drawn. The temporal dynamics in cycle length were assessed by the time and frequency domain properties of

Address for Correspondence: György Kozmann, DSc, Dept. of Information Systems, University of Pannonia, H-8201 PO Box 158., Veszprém, Hungary
Phone: +36 88 624322 Fax: +36 88 624526 E-mail: kozmann@irt.vein.hu

RR time-series. The spatio-temporal dynamics of repolarization disparities were characterized by the Karhunen-Loève (KL) expansion parameters of QRST integral maps, respectively and by the non-dipolarity index (NDI) introduced at the CVRTI, Salt Lake City (13).

Statistical computations (mean-value, standard deviation, auto-, and cross correlation, spectral density, coherence, etc.) were carried out by the STATISTICA program package (StatSoft Inc., Tulsa, OK, USA).

Results

At first, the reproducibility of our results was studied in terms of the Q and T wave-limit determination accuracy. The Q_{onset} time-instant modulation in 5 ms steps around the reference point (up to±10 ms) and the T_{end} modulation in 10 ms steps (up to20 ms) resulted in only minor changes in the KL and in the NDI time-series. The correlation matrix of the reference time-series with the modified series yielded a matrix with nearly unit elements in each matrix position. Consequently, a reasonable error in the wave-limit determination has no significant impact on the results in NDI, and QRST KL plots.

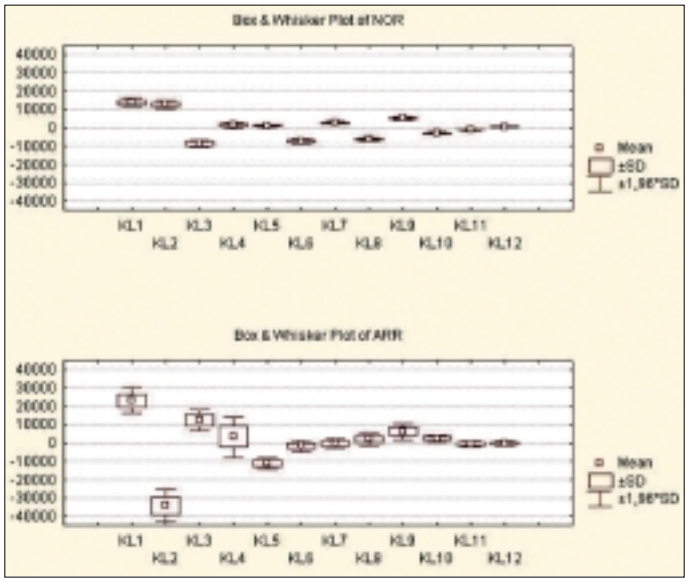

Figure 1. Box and whisker diagrams of the QRST integral KL coefficient variability of a NOR subject (upper) and an ARR patient (lower).

ARR- ventricular arrhythmia patient, KL- Karhunen-Loève expansion parameter, NOR- normal subjects

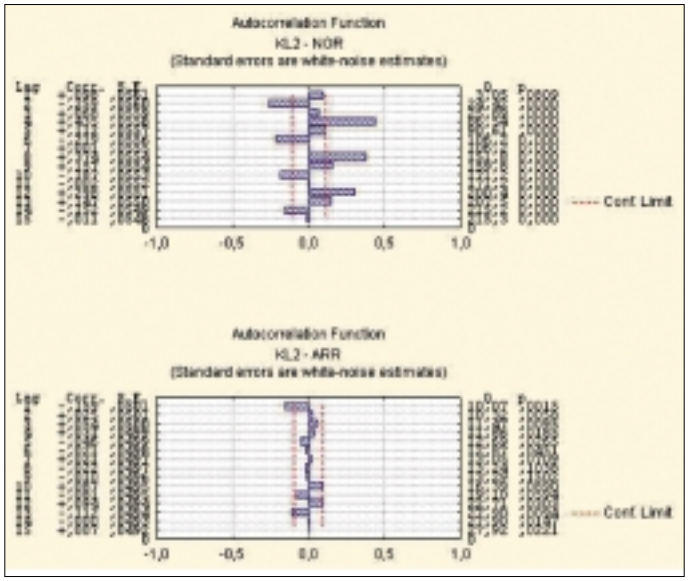

Figure 2. Autocorrelation functions of the 2nd KL coefficients for the same patients as in Figure 1.

KL- Karhunen-Loève expansion parameter

Typical examples of a compact representation of the beat-to-beat QRST pattern changes are shown in Figure 1, in terms of the box and whiskers diagram of the 5-minute-long time-series of the 12 KL coefficients. The examples clearly show, that the variability of ARR patients (lower graph) significantly increased in some of the KL coefficients, i.e. the variability of the subsequent QRST integrals increased compared to the NOR subjects (upper graph). (In the box and whiskers graphs the vertical dimension of the boxes equal two standard deviations, centered on the mean values.)

Correlation matrices of the simultaneously measured KL coefficients (representing the spatial pattern of the individual QRST integral maps) did show marked linear relationships between certain coefficients, especially in normal subjects (upper truncated correlation matrix in Table 1.). The overall level of correlations diminished in patients (lower truncated matrix in Table 1).

Autocorrelation functions at each of the KL time-series exhibited a (respiration related) periodicity in most of our healthy subjects, but a white-noise-like pattern was found in all the ARR patients. Typical examples are shown in Figure 2, for KL2 time-series.

Discussion

QRST integral maps of healthy subjects show a stable pattern along the time coordinate. QRST integral map SD^2/M^2 (amplitude variance/mean signal energy) amplitude values ranged in our sample group between 0.0057-0.008. The spatial distribution of the superimposed beat-to-beat integral map changes was random.

Table 1. Correlation matrices of QRST integral map coefficients (Only the first 6 KL coefficient correlations of the patients shown in Figure 1 are presented)

	KL1	KL2	KL3	KL4	KL5	KL6
KL1	1.00	0.27	-0.07	-0.35	0.14	-0.23
KL2	0.27	1.00	-0.76	0.10	0.59	-0.72
KL3	-0.07	-0.76	1.00	-0.06	-0.48	0.69
KL4	-0.35	0.10	-0.06	1.00	-0.25	-0.23
KL5	0.14	0.59	-0.48	-0.25	1.00	-0.28
KL6	-0.23	-0.72	0.69	-0.23	-0.28	1.00
	KL1	KL2	KL3	KL4	KL5	KL6
KL1	1.00	0.27	0.22	0.02	0.10	0.12
KL2	0.27	1.00	-0.03	0.21	0.49	0.13
KL3	0.22	-0.03	1.00	0.25	0.00	0.07
KL4	0.02	0.21	0.25	1.00	-0.18	0.06
KL5	0.10	0.49	0.00	-0.18	1.00	-0.02
KL6	0.12	0.13	0.07	0.06	-0.02	1.00

KL - Karhunen-Loève expansion parameter

In the group of arrhythmia patients, QRST integral map variability amplitudes increased significantly compared to the healthy group, while the random character of the pattern changes persisted. The QRST integral amplitude SD^2/M^2 values went up to 0.021-0.069.

The correlation matrices of healthy subjects did show significant linear relationship between certain coefficients, but in the examined patients the correlations had a diminishing tendency, suggesting almost independent, random fluctuations in the coefficients, which might be a sign of the weakening resistive electrical coupling in cellular level (14).

Similarly, in normal subjects the autocorrelation functions of the KL components revealed a respiration dependent integral map pattern modulation. However, in ARR cases, the autocorrelation functions of each KL coefficient time-series did show a white-noise-like pattern, the modulation due to respiration was hardly recognizable.

As the integral values in the different leads realize different weightings of the KL components, the QRST integral variability should be different in all chest leads; consequently, the QT length fluctuation should be different in each lead. The surface distribution of fluctuation may identify the anatomical location of the underlying impaired myocardial region.

Conclusions

QRST integral maps provide an insight in the modulation of ventricular repolarization spontaneously or during premature stimuli. The same methodology provides tools for the detailed and non-invasive study of the association of repolarization and depolarization sequences, as well. According to our preliminary findings, map-type studies, but even simplified studies based on NDI parameters offer an unexplored source of information in the study of arrhythmia vulnerability.

Acknowledgements

This study was supported by the National Research Found grants NKFP 2/052/2001, NKFP 2/004/2004 and GVOP-3.1.1-2004-05-0196/3.0. of the Ministry of Education, Hungary.

References

1. Hubley-Kozey CL, Mitchell LB, Gardner MJ, Warren JW, Penney CJ, Smith ER, et al. Spatial features in body-surface potential maps can identify patients with a history of sustained ventricular tachycardia. Circulation 1995; 92: 1825-38.
2. De Ambroggi L, Aime E, Ceriotti C, Rovida M, Negroni S. Mapping of ventricular repolarization potentials in patients with arrhythmogenic right ventricular dysplasia: principal component analysis of the ST-T waves. Circulation 1997; 96: 4314-8.
3. Lombardi F. Chaos theory, heart rate variability, and arrhythmic mortality. Circulation 2000; 101:8-10.
4. Surawicz B. Will QT dispersion play a role in clinical decision-making? J Cardiovasc Electrophysiol 1996; 7: 777-84.
5. Fuller MS, Sandor G, Punske B, Taccardi B, MacLeod RS, Ershler PR, et al. Estimates of repolarization dispersion from electrocardiographic measurements. Circulation 2000; 102: 685-91.
6. Atiga WL, Calkins H, Lawrence JH, Tomaselli GF, Smith JM, Berger RD. Beat-to-beat repolarization lability identifies patients at risk for sudden cardiac death. J Cardiovasc Electrophysiol 1998; 9: 899-908.
7. Burattini L, Zareba W. Time-domain analysis of beat-to-beat variability of repolarization morphology in patients with ischemic cardiomyopathy. J Electrocardiol 1999; 32 Suppl: 166-72.
8. Laurita KR, Girouard SD, Rosenbaum DS. Modulation of ventricular repolarization by a premature stimulus. Circ Res 1996; 79: 493-503.
9. Laurita KR, Girouard SD, Akar FG, Rosenbaum DS. Modulated dispersion explains changes in arrhythmia vulnerability during premature stimulation of the heart. Circulation 1998; 98: 2774-80.
10. Shimizu S, Kobayashi Y, Miyauchi Y, Ohmura K, Atarashi H, Takano T. Temporal and spatial dispersion of repolarization during premature impulse propagation in human intact ventricular muscle: comparison between single vs. double premature stimulation. Europace 2000; 2: 201-6.
11. Geselowitz DB. The ventricular gradient revisited: relation to the area under the action potential. IEEE Trans Biomed Eng 1983; 30: 76-7.
12. Lux RL, Smith CR, Wyatt RF, Abildskov JA. Limited lead selection for estimation of body surface potential maps in electrocardiography. IEEE Trans Biomed Eng 1978; 25: 270-6.
13. Abildskov JA, Green LS, Lux RL. Detection of disparate ventricular repolarization by means of the body surface electrocardiogram. In: Zipes DP, Jalife J, editors. Cardiac Electrophysiology and Arrhythmias. New York: Grune & Stratton; 1985. p. 495-9.
14. Zaniboni M, Pollard AE, Yang L, Spitzer KW. Beat-to-beat repolarization variability in ventricular myocytes and its suppression by electrical coupling. Am J Physiol Heart Circ Physiol 2000; 278: H677-87.